

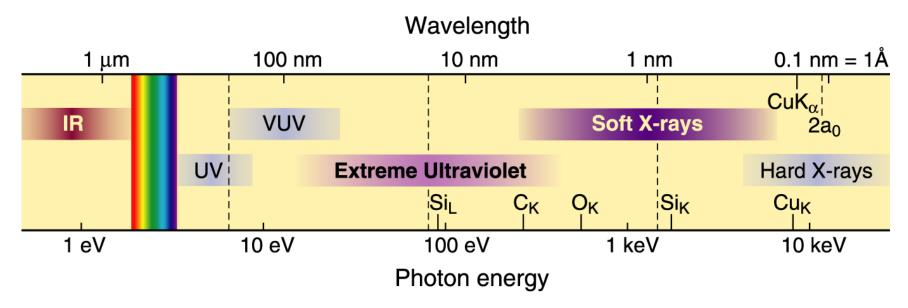
EUV and Soft X-Ray Optics

David Attwood
University of California, Berkeley

Cheiron School September 2013 SPring-8

The short wavelength region of the electromagnetic spectrum





- See smaller features
- Write smaller patterns
- Elemental and chemical sensitivity

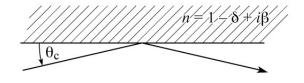
$$\hbar\omega \cdot \lambda = hc = 1239.842 \text{ eV nm}$$

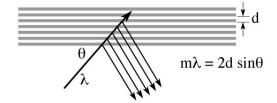
$$n = 1 - \delta + i\beta \qquad \qquad \delta, \, \beta << 1$$

Available x-ray optical techniques

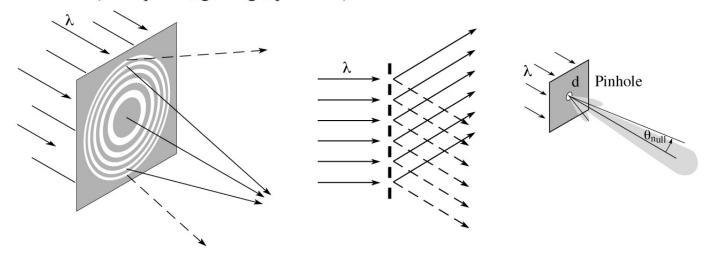


• Reflection (glancing incidence or multilayer coatings)

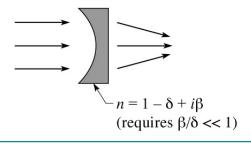


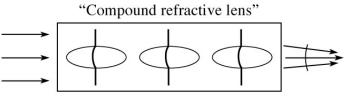


• Diffraction (zone plates, gratings, pinholes)



• Refraction (only for hard x-rays, > 20 keV)





A. Snigerev et al., Nature 384, 49 (7Nov.1996)

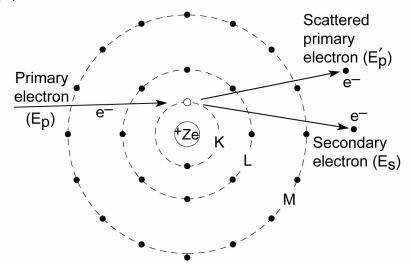
B. Lengeler et al., J. Appl. Phys. <u>84</u>, 5855 (1Dec.1998)

AvailOpticTechSXREUV.ai

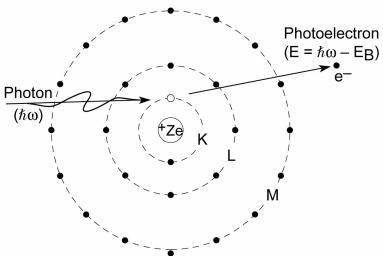
Basic ionization and emission processes in isolated atoms



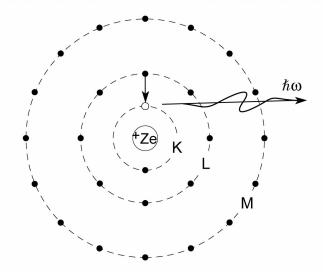
(a) Electron collision induced ionization



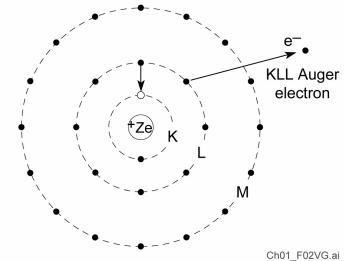
(b) Photoionization



(c) Fluorescent emission of characteristic radiation

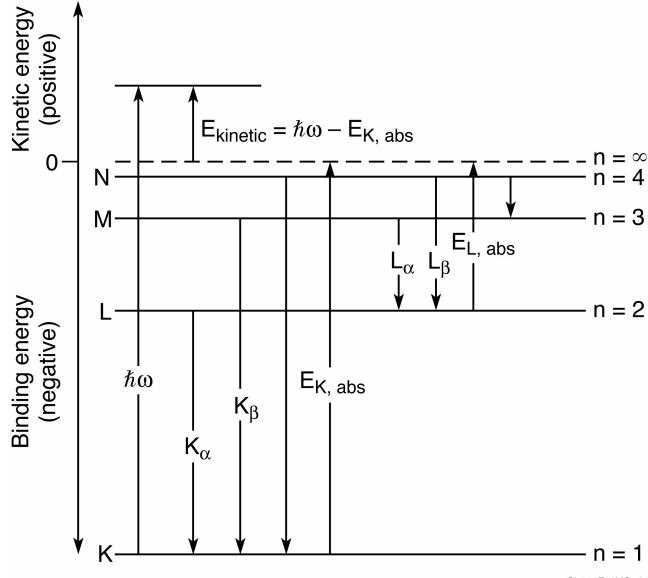


(d) Non-radiative Auger process



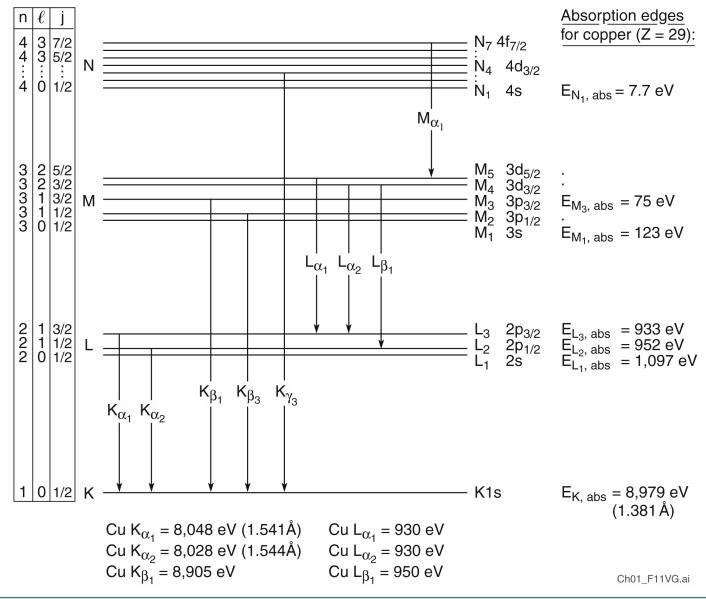
Energy levels, absorption edges, and characteristic line emissions for a multi-electron atom





Energy levels, quantum numbers, and allowed transitions for the copper atom





Refractive index from the IR to x-ray spectral region

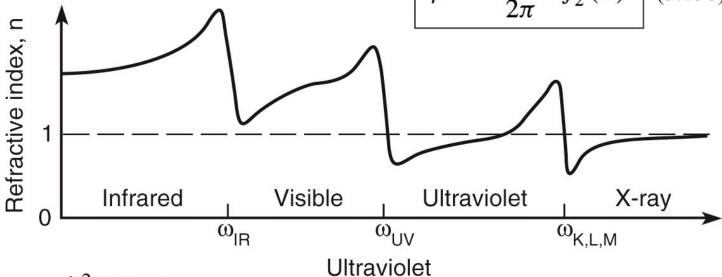


$$n(\omega) = 1 - \delta + i\beta \qquad (3.12)$$

$$\delta = \frac{n_a r_e \lambda^2}{2\pi} f_1^0(\omega) \qquad (3.13a)$$

$$\beta = \frac{n_a r_e \lambda^2}{2\pi} f_2^0(\omega) \qquad (3.13b)$$

$$\beta = \frac{n_a r_e \lambda^2}{2\pi} f_2^0(\omega) \quad (3.13b)$$



- λ^2 behavior
- δ & β << 1
- δ -crossover

Ch03_RefrcIndxIR.XR.ai

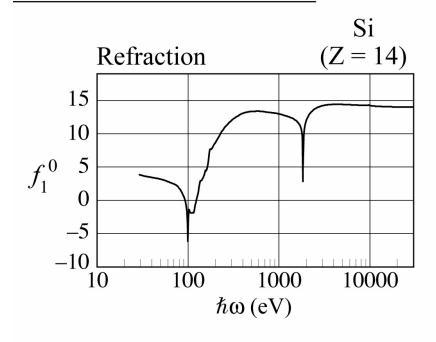
Refractive index at nanometer wavelengths

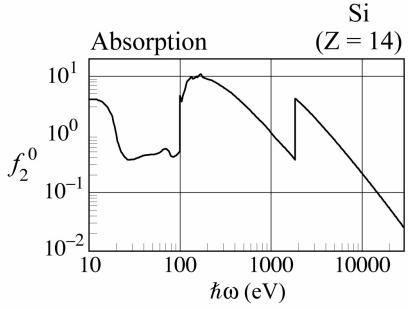


Refractive Index

$$n = 1 - \delta + i\beta = 1 - \frac{n_a r_e \lambda^2}{2\pi} (f_1^0 - i f_2^0)$$

Atomic scattering factors





ScattrngRefracIndex_June2009.ai

Refractive index in the soft x-ray and EUV spectral region



$$n(\omega) = 1 - \frac{1}{2} \frac{e^2 n_a}{\epsilon_0 m} \sum_s \frac{g_s}{\left(\omega^2 - \omega_s^2\right) + i\gamma\omega}$$
 (3.8)

Noting that

$$r_e = \frac{e^2}{4\pi \epsilon_0 mc^2}$$

and that for forward scattering

$$f^{0}(\omega) = \sum_{s} \frac{g_{s}\omega^{2}}{\omega^{2} - \omega_{s}^{2} + i\gamma\omega}$$

where this has complex components

$$f^0(\omega) = f_1^0(\omega) - i f_2^0(\omega)$$

The refractive index can then be written as

$$n(\omega) = 1 - \frac{n_a r_e \lambda^2}{2\pi} \left[f_1^0(\omega) - i f_2^0(\omega) \right]$$
 (3.9)

which we write in the simplified form

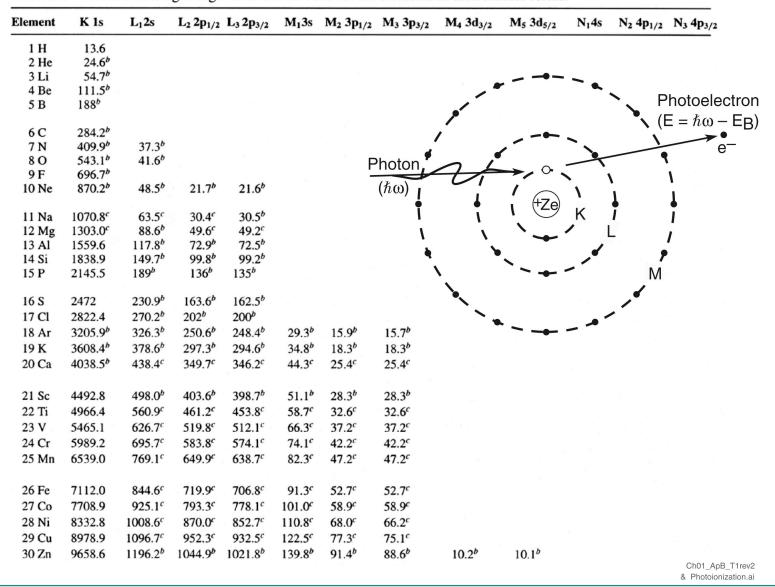
$$n(\omega) = 1 - \delta + i\beta \tag{3.12}$$

Ch03_RefracIndex2.ai

Photoionization and electron binding energies



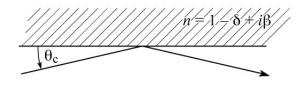
TABLE B.1. Electron binding energies in electron volts for the elements in their natural forms.^a

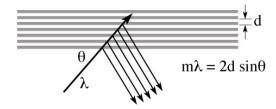


Available x-ray optical techniques

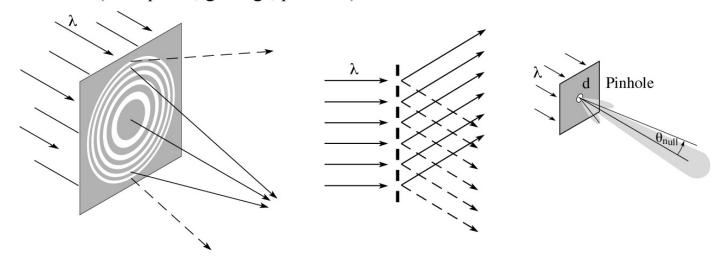


• Reflection (glancing incidence or multilayer coatings)

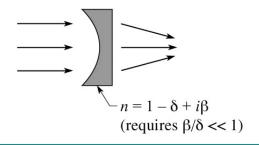


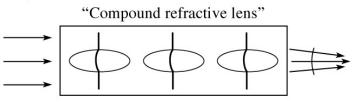


• Diffraction (zone plates, gratings, pinholes)



• Refraction (only for hard x-rays, > 20 keV)



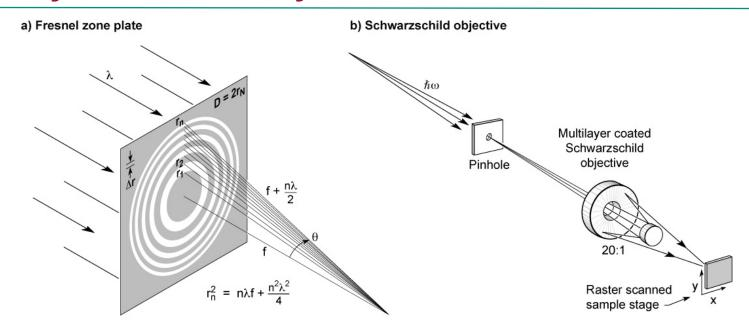


- A. Snigerev et al., Nature 384, 49 (7Nov.1996)
- B. Lengeler et al., J. Appl. Phys. <u>84</u>, 5855 (1Dec.1998)

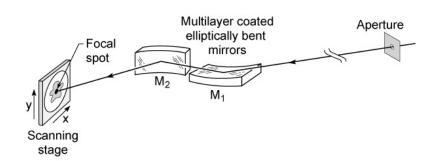
AvailOpticTechSXREUV.ai

Diffractive and reflective optics for EUV, soft x-rays and hard x-rays

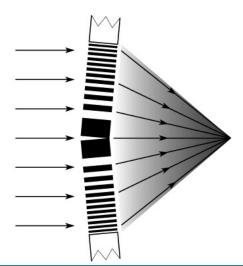




c) Kirkpatrick-Baez mirror pair



d) Multilayer Laue lens



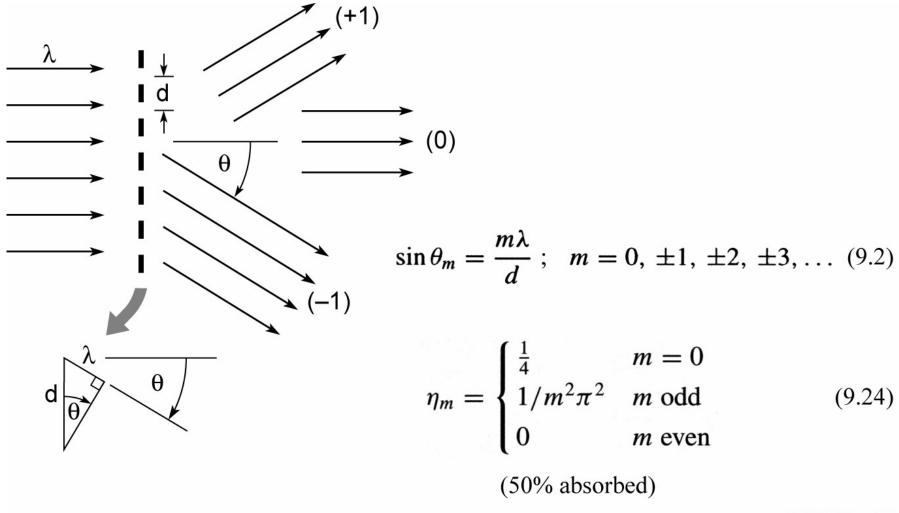
Diffractive optics for soft x-rays and EUV



Zone Plates Gratings Pinholes A Pinhole DiffracOptics.ai

Diffraction from a transmission grating

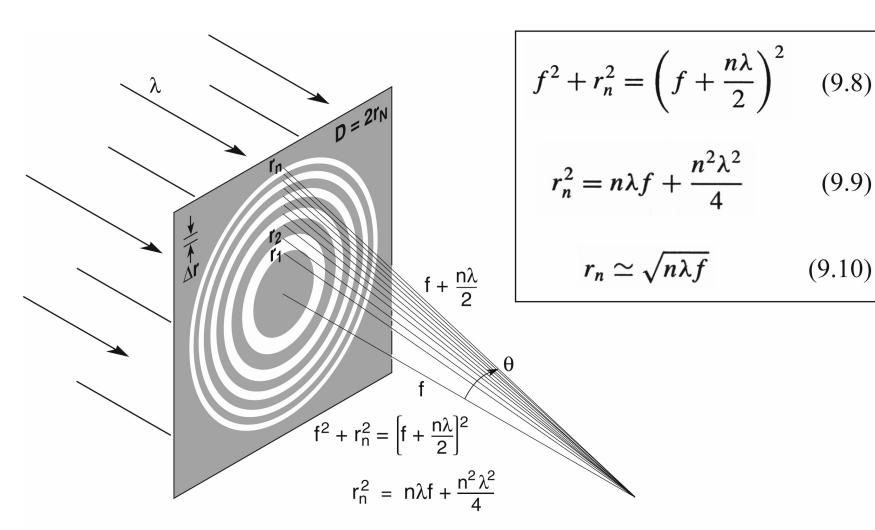




Ch09 F03VGrev.4.04.ai

A Fresnel zone plate lens

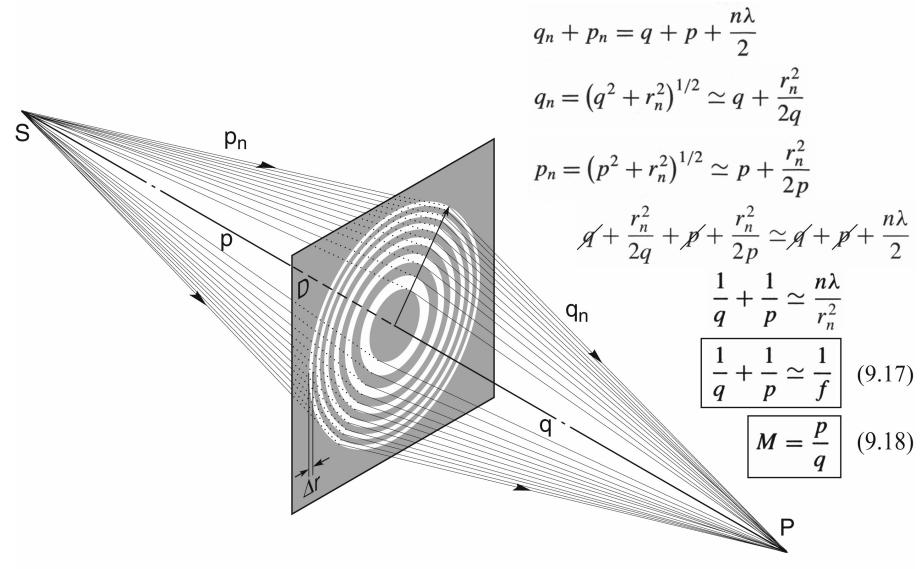




Ch09_F05VG.ai

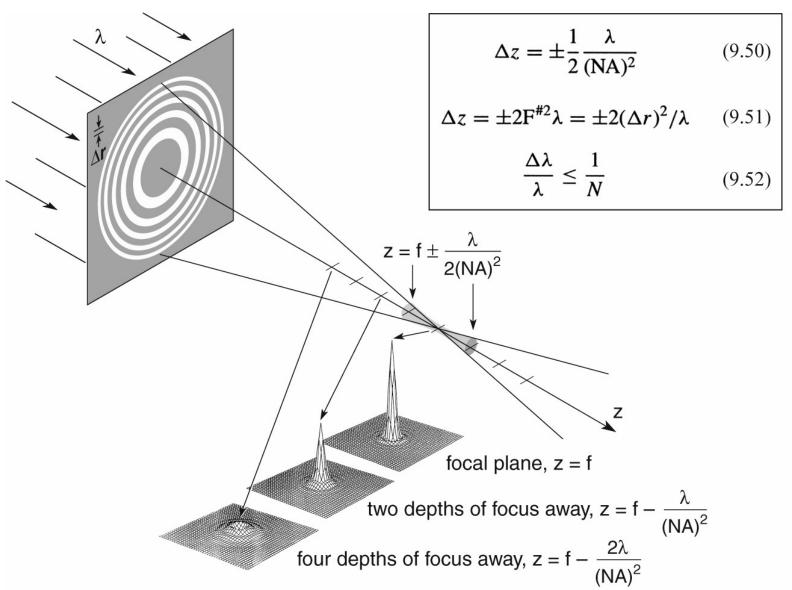
A Fresnel zone plate lens used as a diffractive lens for point to point imaging





Depth of focus and spectral bandwidth

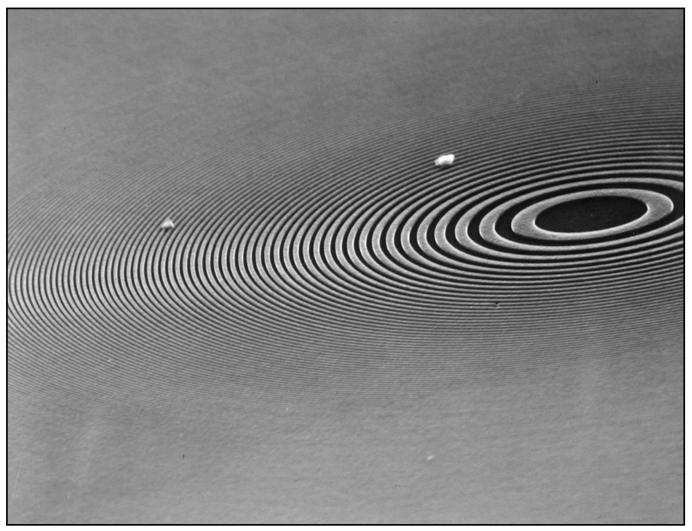






A Fresnel zone plate lens for soft x-ray microscopy





Courtesy of E. Anderson, LBNL

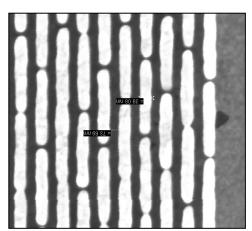


Zone plates for ALS STXM beamlines – "3D Engineered Nanostructures"

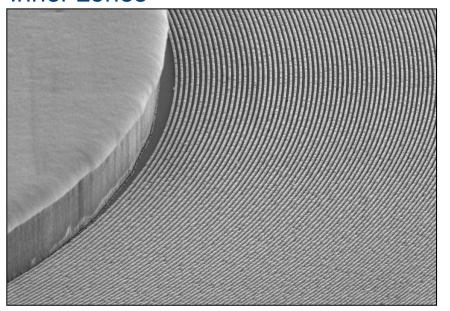


 $\Delta r = 35 \text{ nm}, \ \Delta t = 180 \text{ nm Au}, \ N = 1700 \ D = 240 \ \mu\text{m}, \ 3 \ x \ 95 \ \mu\text{m}^{D} \ \text{central stop}$

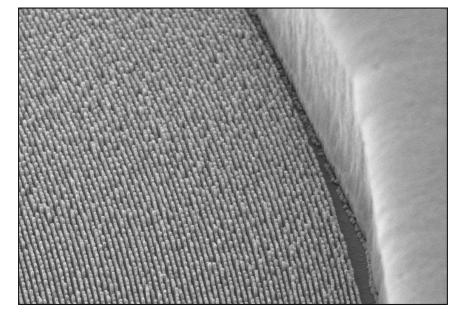
Outer zone close-up



Inner zones



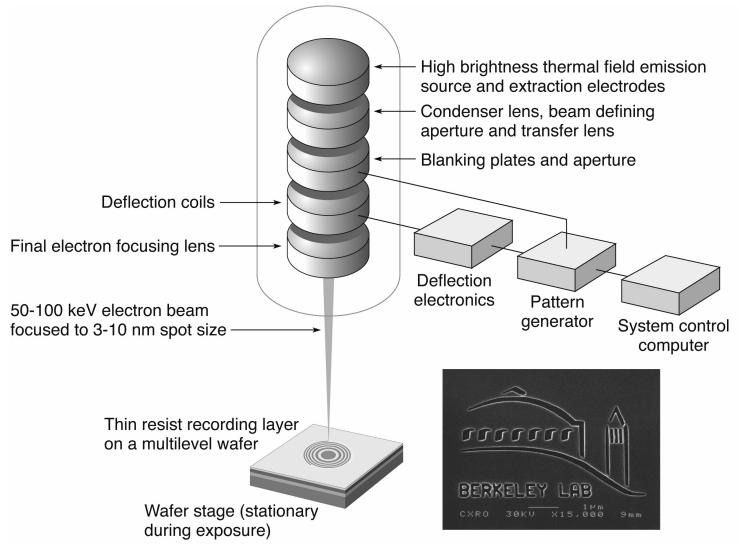
Outer zones





The Nanowriter: high resolution electron beam writing with high placement accuracy





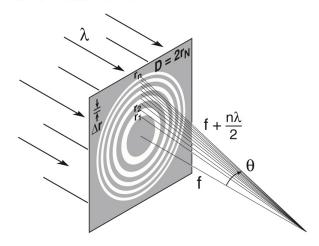
Ch09_F43VG.ai

Courtesy of E. Anderson (LBNL)

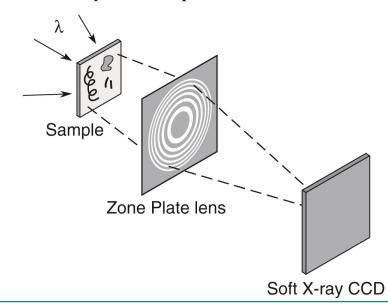
Zones plates for soft x-ray image formation



Zone Plate Lens



Soft X-Ray Microscope



Zone Plate Formulae

$$r_n^2 = n\lambda f + \frac{n^2\lambda^2}{4}$$
 (9.9)
$$\lambda = 2.5 \text{ nm},$$
$$\Delta r = 25 \text{ nm}$$
$$N = 618$$

$$D = 4N\Delta r \tag{9.13}$$

$$f = \frac{4N(\Delta r)^2}{\lambda}$$
 (9.14) 0.63 mm

$$NA = \frac{\lambda}{2\Lambda r} \tag{9.15}$$

Res. =
$$k_1 \frac{\lambda}{NA} = 2k_1 \Delta r$$

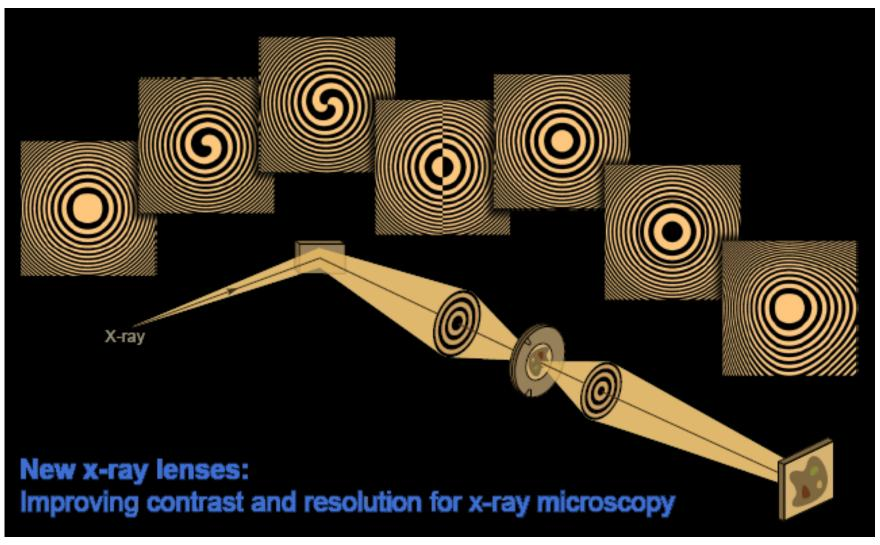
$$\begin{cases} k_1 = 0.61 \\ (\sigma = 0) \end{cases}$$
 1.22 $\Delta r = 30 \text{ nm}$
$$\begin{cases} k_1 = 0.4 \\ (\sigma = 0.45) \end{cases}$$
 0.8 $\Delta r = 19 \text{ nm}$

DOF =
$$\pm \frac{1}{2} \frac{\lambda}{(NA)^2}$$
 (9.50) 1 μm

$$\frac{\Delta\lambda}{\lambda} \le \frac{1}{N} \tag{9.52}$$

New x-ray lenses: Improving contrast and resolution for x-ray microscopy



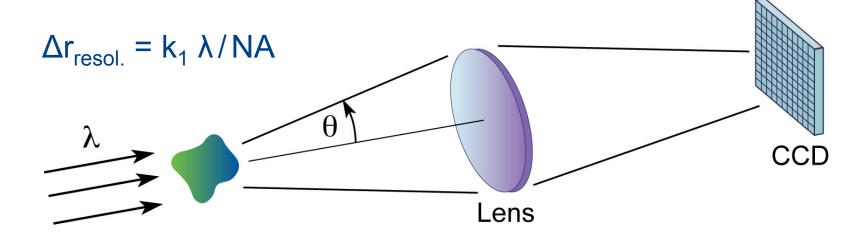


C. Chang, A. Sakdinawat, P.J. Fischer, E.H. Anderson, D.T. Attwood, Opt. Lett. 2006; Sakdinawat and Liu, Opt. Lett. 2007; Sakdinawat and Liu, Opt. Express 2008

Diffraction limited x-ray imaging



Diffraction limited imaging is limited by the finite wavelength and acceptance aperture:



where NA = $n \sin\theta$ and the constant k_1 depends on illumination and specific image modulation criteria. For x-rays

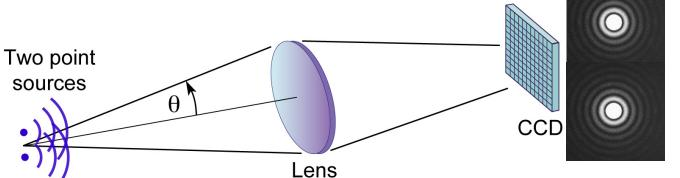
$$n = 1 - \delta + i\beta$$
 $\delta, \beta << 1$

$$\delta$$
, β << 1

Diffraction limited x-ray imaging

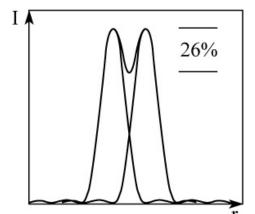


For example, the widely accepted Rayleigh criteria for resolving two adjacent, mutually incoherent, point sources of light, results in a 26% intensity modulation.



 $\lambda = 2.48 \text{ nm}$ (500 eV)

Two overlapping Airy patterns



 $\Delta r_{resol.} = 0.61 \lambda / NA$

Resultant intensity pattern when the two point sources are "just resolved", such that the central lobe maximum due to one point source overlaps the first minimum (dark ring) of the other.

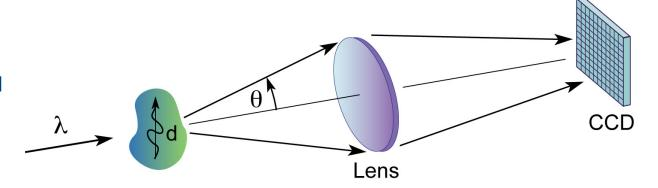
Note: Other definitions are possible, depending on the application and the ability to discern separated objects.

Resolution and illumination

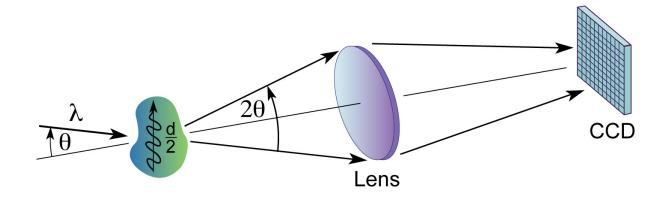


Achievable resolution can be improved by varying illumination:

An object pattern of periodicity d diffracts light and is just captured by the lens – setting the diffraction limited resolution limit.

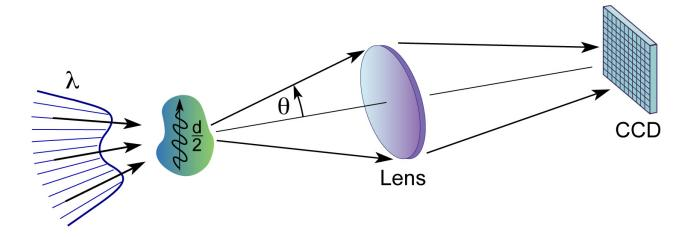


Diffraction from an object of smaller periodicity, d/2, is just captured, and resolved, when illuminated from an angle.

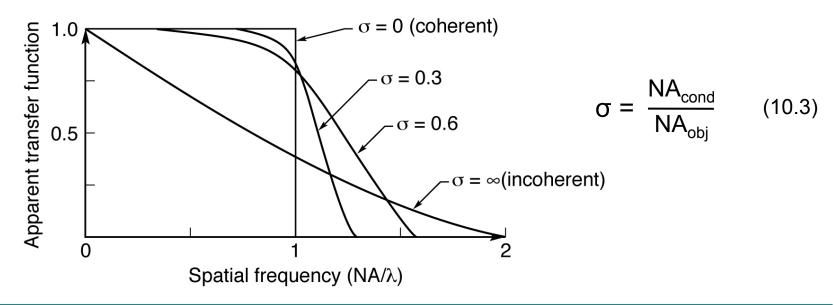


Resolution, illumination, and optical transfer function





Spatial frequency response of the optical system can be optimized by tailoring the angular distribution of illumination.





LETTERS



Soft X-ray microscopy at a spatial resolution better than 15 nm

Weilun Chao^{1,2}, Bruce D. Harteneck¹, J. Alexander Liddle¹, Erik H. Anderson¹ & David T. Attwood^{1,2}

Analytical tools that have spatial resolution at the nanometre scale are indispensable for the life and physical sciences. It is desirable that these tools also permit elemental and chemical identification on a scale of 10 nm or less, with large penetration depths. A variety of techniques1-7 in X-ray imaging are currently being developed that may provide these combined capabilities. Here we report the achievement of sub-15-nm spatial resolution with a soft X-ray microscope—and a clear path to below 10 nm—using an overlay technique for zone plate fabrication. The microscope covers a spectral range from a photon energy of 250 eV (~5 nm wavelength) to 1.8 keV (~0.7 nm), so that primary K and L atomic resonances of elements such as C, N, O, Al, Ti, Fe, Co and Ni can be probed. This X-ray microscopy technique is therefore suitable for a wide range of studies: biological imaging in the water window^{8,9}; studies of wet environmental samples10,11; studies of magnetic nanostructures with both elemental and spin-orbit sensitivity12-14; studies that require viewing through thin windows, coatings or substrates (such as buried electronic devices in a silicon chip¹⁵); and three-dimensional imaging of cryogenically fixed biological cells9,16.

The microscope XM-1 at the Advanced Light Source (ALS) in Berkeley¹⁷ is schematically shown in Fig. 1. The microscope type is similar to that pioneered by the Göttingen/BESSY group (ref. 18, and references therein). A 'micro' zone plate (MZP) projects a full-field image to an X-ray-sensitive CCD (charge-coupled device), typically in one or a few seconds, often with several hundred images per day. The field of view is typically 10 μm , corresponding to a magnification of 2,500. The condenser zone plate (CZP), with a central stop, serves two purposes in that it provides partially coherent hollow-cone illumination², and, in combination with a pinhole, serves as the

Source Condenser Objective

Condenser zone plate
Plane mirror

ALS bending magnet

Micro zone plate
Soft x-ray sensitive CCD

Figure 1 | A diagram of the soft X-ray microscope XM-1. The microscope uses a micro zone plate to project a full field image onto a CCD camera that is sensitive to soft X-rays. Partially coherent, hollow-cone illumination of the sample is provided by a condenser zone plate. A central stop and a pinhole provide monochromatization.

monochromator. Monochromatic radiation of $\lambda/\Delta\lambda = 500$ is used. Both zone plates are fabricated in-house, using electron beam lithography¹⁹.

The spatial resolution of a zone plate based microscope is equal to $k_1 \lambda N k_{MZP}$ where λ is the wavelength, $N k_{MZP}$ is the numerical aperture of the MZP, and k_1 is an illumination dependent constant, which ranges from 0.3 to 0.61. For a zone plate lens used at high magnification, $N k_{MZP} = \mathcal{M} 2 \lambda r_{MZP}$ where $k_{MZP} = k_{MZP} = k_$

This technique overcomes nanofabrication limits due to electron beam broadening in high feature density patterning. Beam broadening results from electron scattering within the recording medium (resist), leading to a loss of image contrast and thus resolvability for $\lambda = 1.52 \text{ nm } (815 \text{ eV})$

 $\Delta r = 15 \text{ nm}$

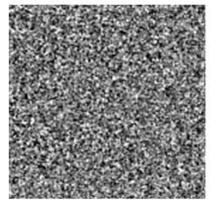
N = 500

 $D = 30 \mu m$

 $f = 300 \mu m$

 $\sigma = 0.38$

 $0.8 \Delta r = 12 \text{ nm}$



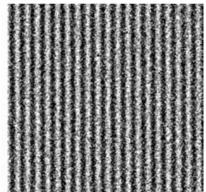


Figure 4 \mid Soft X-ray images of a 15.1 nm half-period test object , as formed with zone plates having outer zone widths of 25 nm and 15 nm.

¹Center for X-ray Optics, Lawrence Berkeley National Laboratory, 1 Cyclotron Road, MS 2-400, ²Department of Electrical Engineerin California, Berkeley, California 94720, USA.

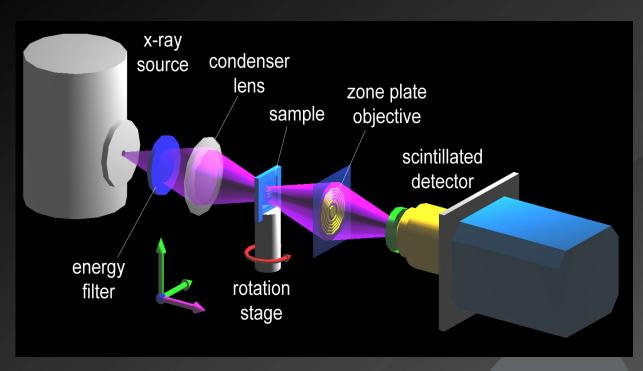
Cr/Si test pattern (Cr L₃ @ 574 eV) (2000 X 2000, 10⁴ ph/pixel)

Hard x-ray zone plate microscopy



- Shorter wavelengths, potentially better spatial resolution and greater depth-of-field.
- Less absorption (β); phase shift (δ) dominates, higher efficiency.
- Thicker structures required (e.g., zones), higher aspect ratios pose nanofabrication challenges.
- Contrast of nanoscale samples minimal; will require good statistics, uniform background, dose mitigation.

Nanoscale hard x-ray tomography





Challenges for achieving nm scale resolution:

- High resolution objective lens: limiting the ultimate resolution
- High numerical aperture condenser lens:
- Detector: high efficiency for lab. source and high speed for synchrotron sources
- Precision mechanical system

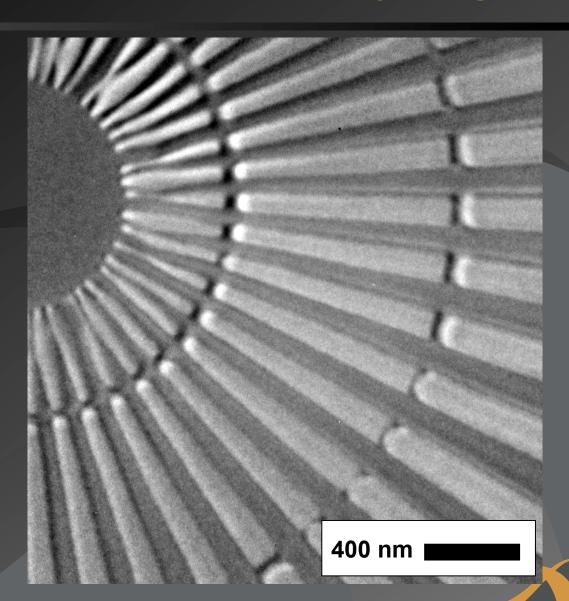
Xradia nanoXCT: Sub-25 nm Hard X-ray Image

Xradia Resolution Pattern

- 50 nm bar width
- 150 nm thick Au
- 8keV x-ray energy
- 3rd diffraction order

F. Duewer, M. Tang, G. C. Yin, W. Yun, M. Feser, et al.

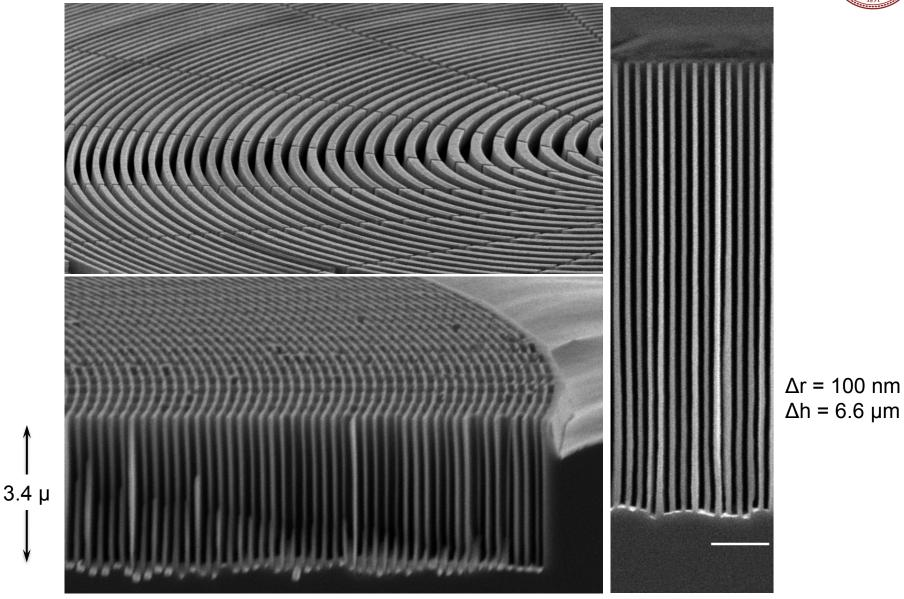
Xradia nano-XCT 8-50S installed at NSRRC, Taiwan





New ultra high aspect ratio, high efficiency, hard x-ray zone plates for high spatial resolution at 30-50 keV



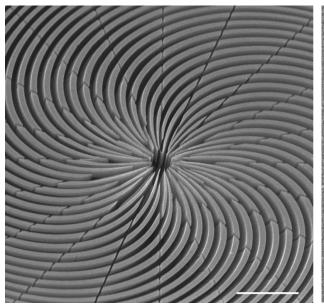


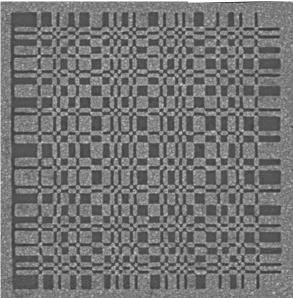
Courtesy of Anne Sakdinawat and Chieh Chang (SLAC)

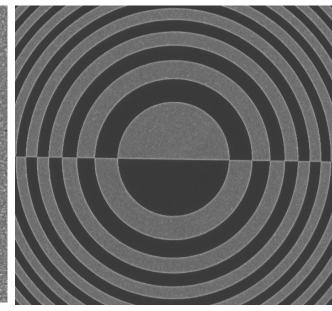


Specialized x-ray diffractive optical elements enable new science at synchrotron facilities









Spiral zone plate for producing x-rays with charge 50 orbital angular momentum

Uniformly redundant array for x-ray parallel holography, alignment, and other applications

Zone plate for x-ray differential interference contrast microscopy

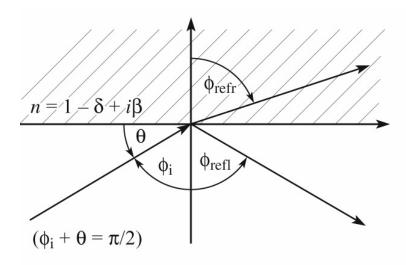
Hard x-ray imaging based on glancing incidence reflective optics

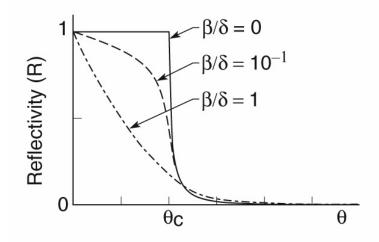


- Optics behave differently at these very short wavelengths (nanometers rather than 520 nm green light)
- The refractive index is less than unity, $n = 1 \delta + i\beta$
- Waves bend away form the normal at an interface
- Absorption is significant in all materials and at all wavelength.
- Because of absorption, refractive lenses do not work, prisms do not, windows need to be extremely thin (100 nm or less).
- Because light is bent away from the surface normal, it possible to have "total external reflection" at glancing incidence – a commonly used technique.
- Kirkpatrick-Baez (KB) mirror pair

Glancing incidence optics







Snell's Law:

$$Sin \ \phi_{refr.} = \frac{Sin \ \phi_i}{n}$$

Total external Reflection:

$$\phi_{refr.} \rightarrow \frac{\pi}{2} \text{ as } \phi_i \rightarrow \phi_{critical}$$

Snell's Law:
$$1 = \frac{\sin \phi_c}{1 - \delta}$$

$$Sin(90^{\circ} - \theta_{c}) = 1 - \delta$$

$$\cos \theta_c = 1 - \delta$$

$$1 - \frac{\theta_c^2}{2} = 1 - \delta$$

$$\theta_{\rm c} = \sqrt{2\delta}$$

For gold at 1 keV

$$\delta = 2.1 \times 10^{-3}$$

$$\theta_{\rm c} = 3.7^{\circ}$$

www.cxro.LBL.gov;

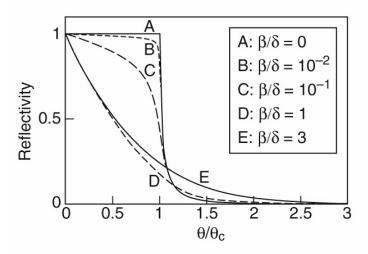
"X-ray properties of the elements"

"X-ray interaction with matter"

Total external reflection with finite β

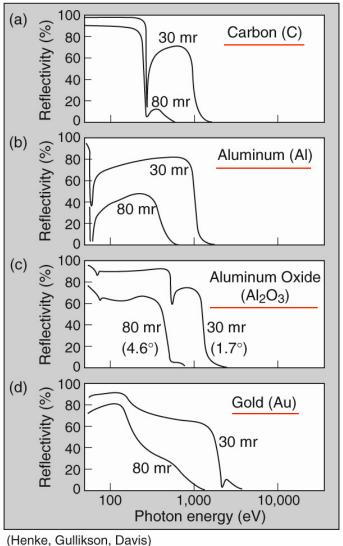


Glancing incidence reflection as a function of β/δ



- finite β/δ rounds the sharp angular dependence
- cutoff angle and absorption edges can enhance the sharpness
- note the effects of oxide layers and surface contamination

... for real materials



Ch03 TotalExtrnlReflc3.ai

Normal incidence reflection at an interface



$$R_s = \frac{\left|\cos\phi - \sqrt{n^2 - \sin^2\phi}\right|^2}{\left|\cos\phi + \sqrt{n^2 - \sin^2\phi}\right|^2}$$
(3.49)

at $\phi = 0$:

$$R_{s,\perp} = \frac{|1-n|^2}{|1+n|^2} = \frac{(1-n)(1-n^*)}{(1+n)(1+n^*)}$$

For $n = 1 - \delta + i\beta$

$$R_{s,\perp} = \frac{(\delta - i\beta)(\delta + i\beta)}{(2 - \delta + i\beta)(2 - \delta - i\beta)} = \frac{\delta^2 + \beta^2}{(2 - \delta)^2 + \beta^2}$$

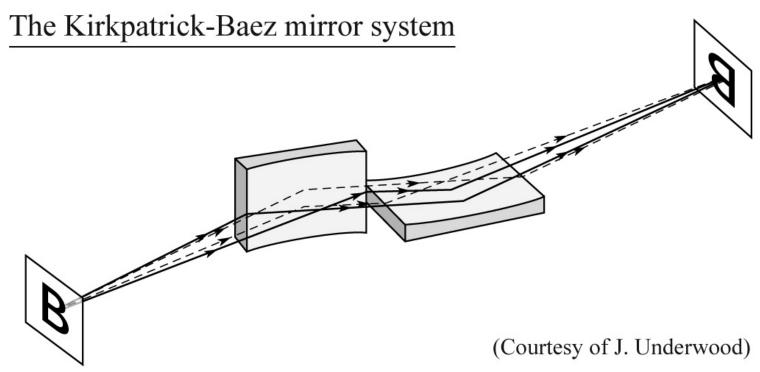
Reflectivity for x-ray and EUV radiation at normal incidence ($\phi = 0$):

$$R_{s,\perp} \simeq \frac{\delta^2 + \beta^2}{4} \tag{3.50}$$

$$\begin{array}{ccc} \underline{Example:} & \text{Nickel } @ \ 300 \ eV \ (4.13 \ nm) \\ & f_1^\circ = 17.8 & f_2^\circ = 7.70 \\ & \delta = 0.0124 & \beta = 0.00538 \end{array} \right\} \ R_\perp = 4.58 \times 10^{-5}$$

Focusing with curved glancing incidence optics





- Two crossed cylinders (or ellipses)
- Astigmatism cancels
- Common use in synchrotron radiation beamlines
- Hard x-ray microprobe



Fluorescent microprobe based in crossed cylinders



Synchrotron Source (white radiation)

Kirkpatrick-Baez (KB) optics

Sample Focal elliptically bent mirrors

Multilayer coated elliptically bent mirrors

(Courtesy of A. Thompson and J. Underwood, LBNL; and R. Holm, Miles Lab)

Fluorescent x-rays

- Crossed cylinders at glancing incidence
- Ellipses better

Scanning

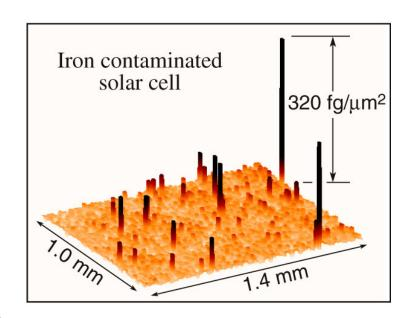
stage

- Photon in / photon out, low noise background
- Femtogram and part per billion (ppb) sensitivity
- Sub-micron focus (to 0.1 μm recently), but scattering gives several micron "50% encircled energy"

Solid state

Si (Li) detector

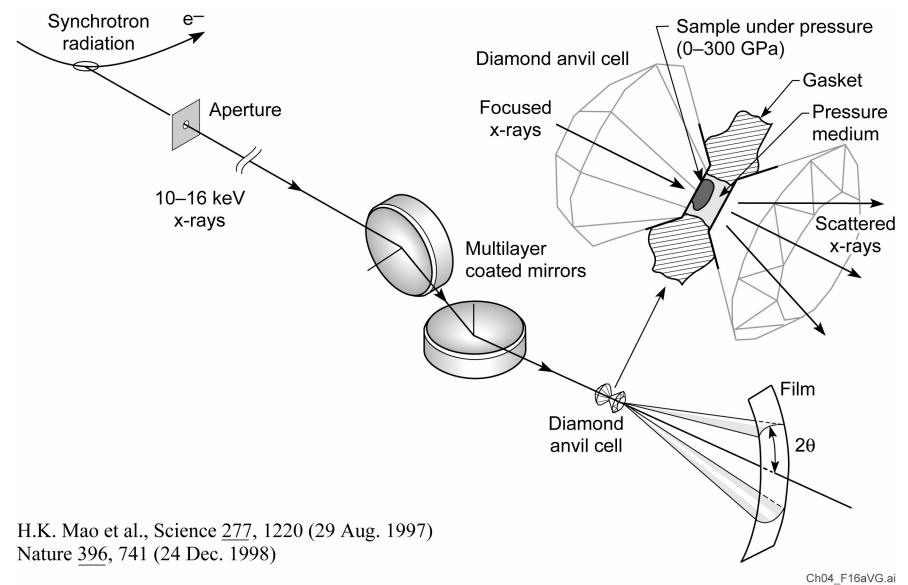
• K-B optics have many applications to synchrotron beamlines, fusion diagnostics, etc.



Aperture

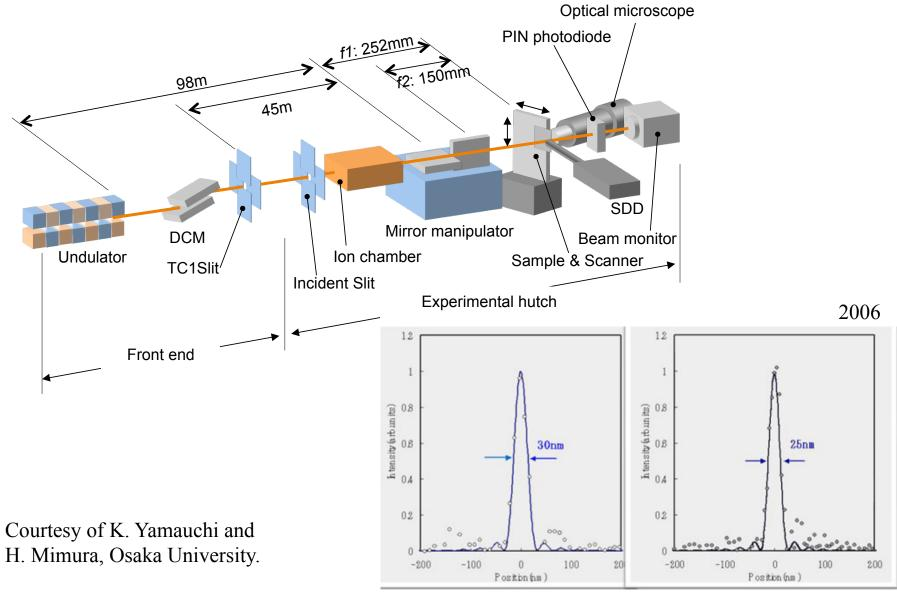
High resolution x-ray diffraction under high pressure using multilayer coated focusing optics





X-ray microprobe at SPring-8

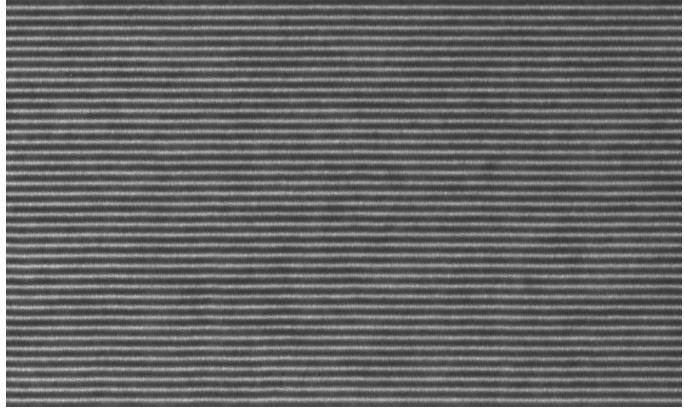




A high quality Mo/Si multilayer mirror



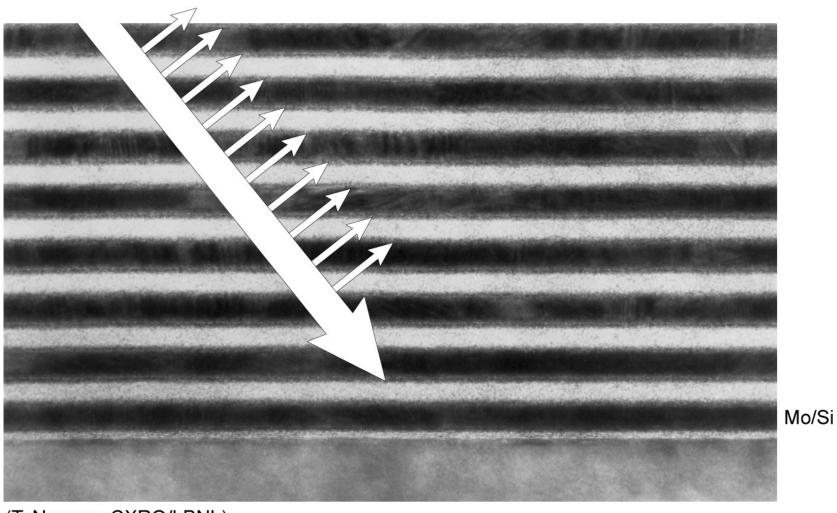
$$N = 40$$
$$d = 6.7$$



Courtesy of Saša Bajt (LLNL)

Scattering by density variations within a multilayer coating



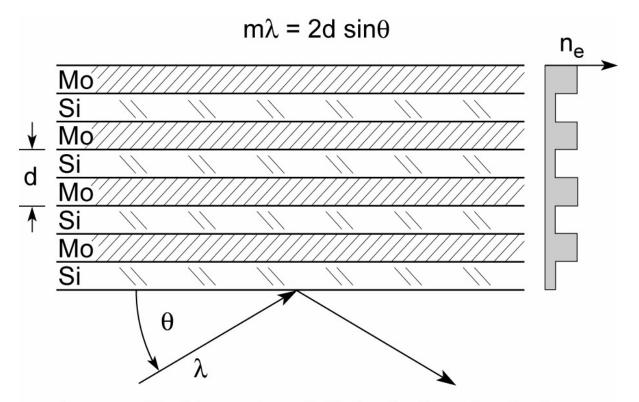


(T. Nguyen, CXRO/LBNL)

Ch04_F01_Feb2007.ai

Multilayer mirrors satisfy the Bragg condition





For normal incidence, $\theta = \pi/2$, first order (m = 1) reflection

$$\lambda = 2d$$

$$d = \lambda/2$$

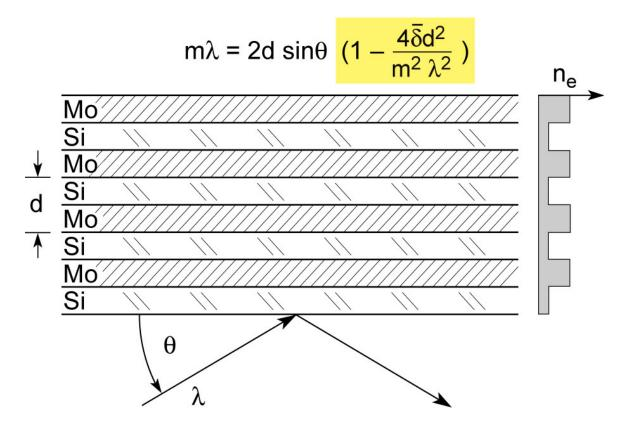
if the two layers are approximately equal

$$\Delta t \simeq \lambda/4$$

a quarter-wave plate coating.

Multilayer mirrors satisfy the Bragg condition





For normal incidence, $\theta = \pi/2$, first order (m = 1) reflection

$$\lambda = 2d$$

$$d = \lambda/2$$

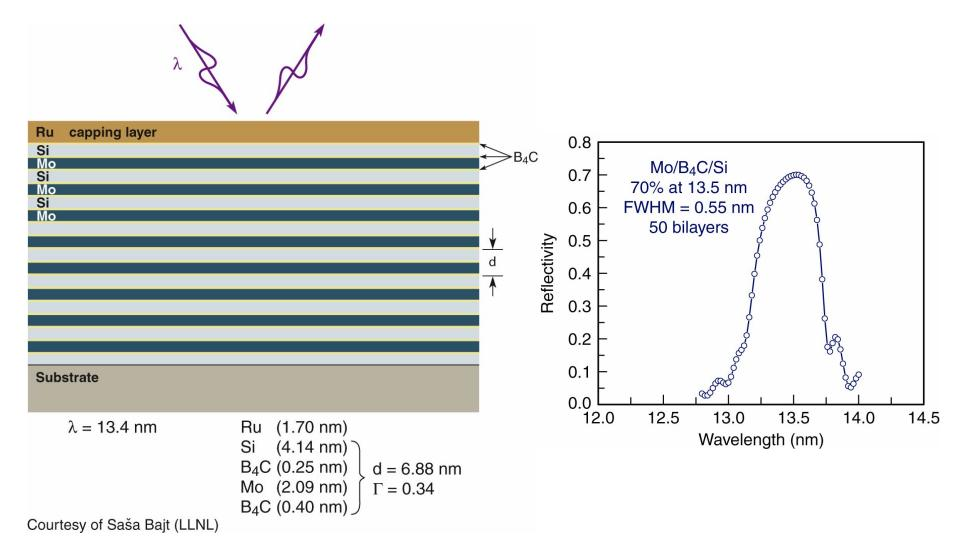
if the two layers are approximately equal

$$\Delta t \simeq \lambda/4$$

a quarter-wave plate coating.

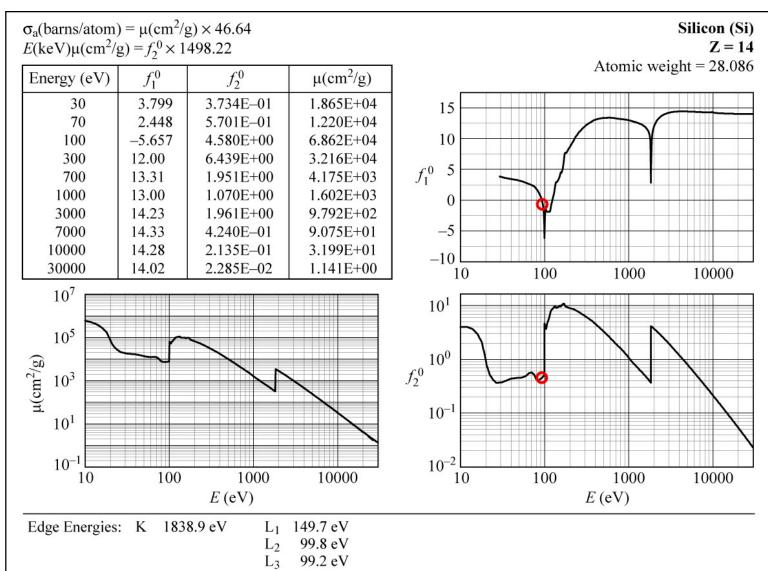
High reflectivity, thermally and environmentally robust multilayer coatings for high throughput EUV lithography





Atomic scattering factors for silicon (Z = 14)

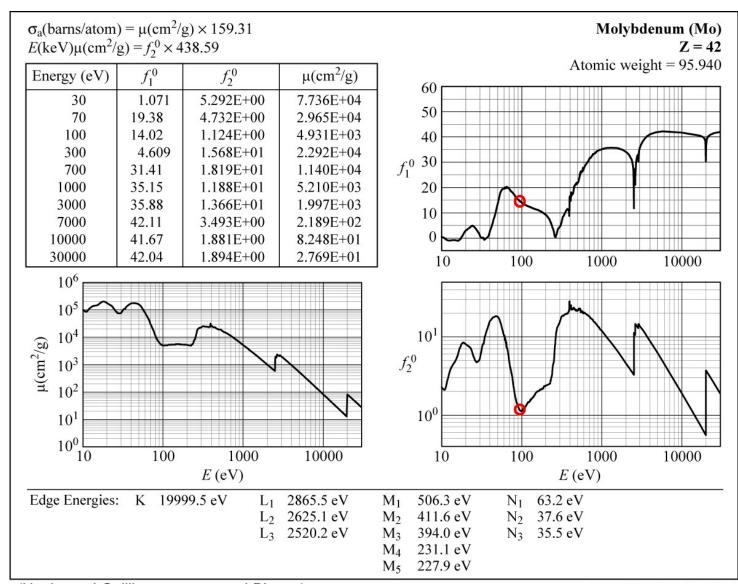




(Henke and Gullikson; www-cxro.LBL.gov)

Atomic scattering factors for molybdenum (Z = 42)





(Henke and Gullikson; www-cxro.LBL.gov)

Ch02ApC Tb1F12 June2008.ai

CXRO Web Site





X-Ray Interactions with Matter . Search CXRO

Facilities

Publications

Research

X-Ray Tools

Visitors

Personnel

Comments?

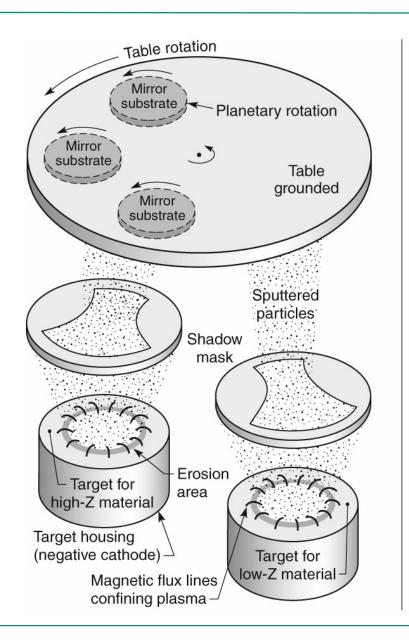
Server Stats

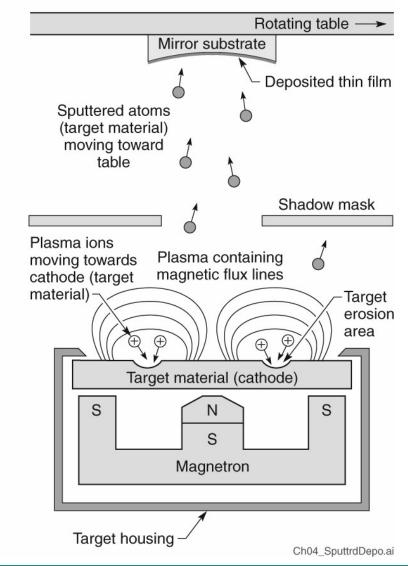
www.cxro.LBL.gov/

- Atomic scattering factors
- EUV/x-ray properties of the elements
- Index of refraction for compound materials
- Absorption, attenuation lengths, transmission
- EUV/x-ray reflectivity (mirrors, thin films, multilayers)
- Transmission grating efficiencies
- Multilayer mirror achievements
- Other

Sputtered deposition of a multilayer coating









Multilayer coatings – "1D nanostructures"

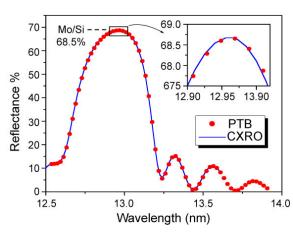


Eric Gullikson, Farhad Salmassi, Yanwei Liu, Andy Aquila (grad), Franklin Dollar (UG)

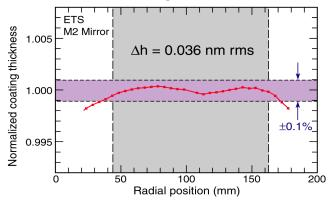




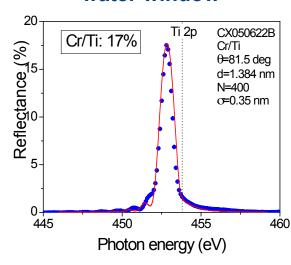
World reference standard



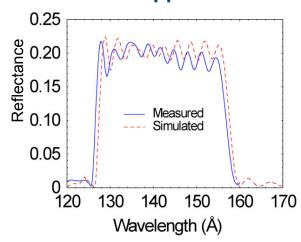
Creating uniformity for $\lambda/50$ optics



World record in water window



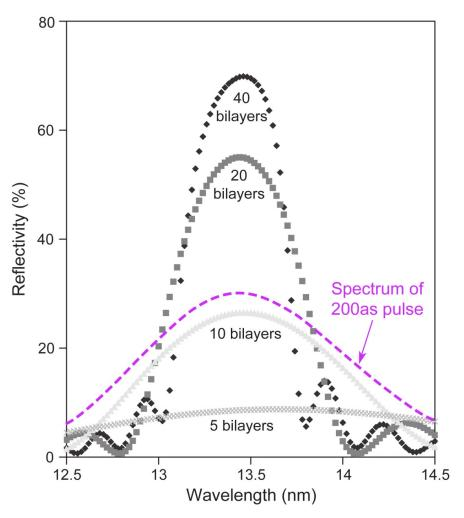
Wide band, narrow band, and chirped mirrors for fsec applications



Broad bandwidth mirrors needed for as/fs pulses



$\Delta E(eV) \cdot \Delta \tau(fs) \ge 1.8 \text{ fs} \cdot eV \text{ (FWHM)}$



- Multilayer mirrors depend on constructive interference from individual interfaces
- Higher reflectivity needs more layers
- Bandwidth gets narrower with more layers

Attosecond pulse

- → Broad bandwidth
- → Limited number of layers

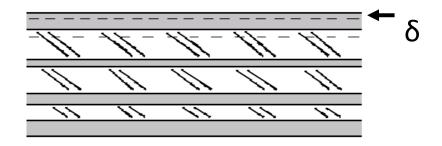
N<10 layers required for 200 as pulse (@13nm)

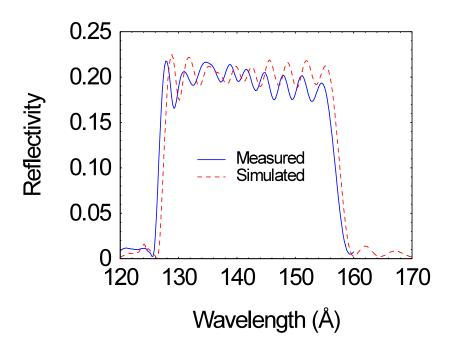


Aperiodic multilayers for asec application



Optimizing multilayers for specific applications requires the use of simulation of a multilayer stack with variations in the thickness of each material in the multilayer.





Successful design of aperiodic multilayers requires:

- 1. EM wave in multilayer structure
- 2. Optimization Algorithm
- 3. Sample preparation
- 4. Verification

A. L. Aquila, F. Salmassi, F. Dollar, Y. Liu, and E. Gullikson, "Developments in realistic design for aperiodic Mo/Si multilayer mirrors," Opt. Express 14, 10073-10078 (2006)

The Cassegrain Telescope with multilayer coatings for EUV imaging of the solar corona



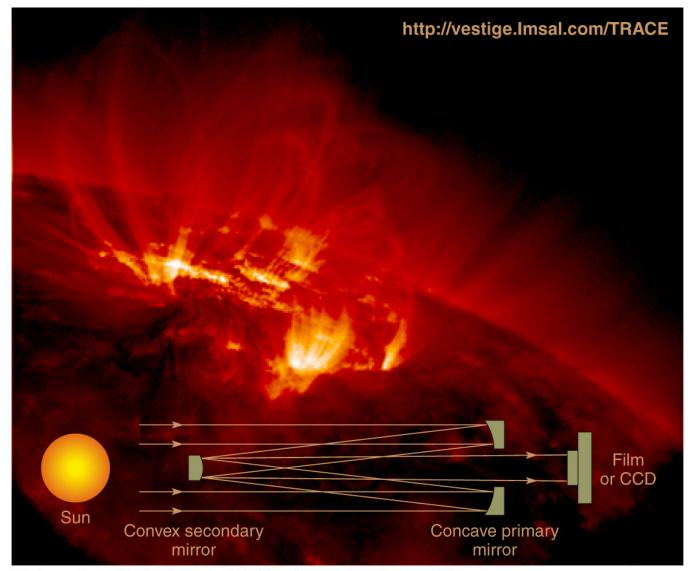


(Photo courtesy of L.Golub, Harvard-Smithsonian and T. Barbee, LLNL)

Photon energy, wavelength, power



$$\hbar\omega \cdot \lambda = hc = 1239.842 \text{ eV nm}$$

(1.1)

1 joule
$$\Rightarrow 5.034 \times 10^{15} \lambda [nm]$$
 photons

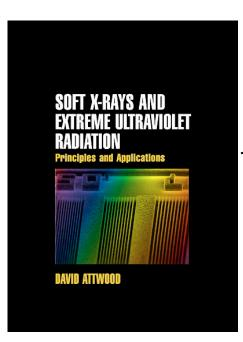
(1.2a)

1 watt
$$\Rightarrow 5.034 \times 10^{15} \lambda [\text{nm}] \frac{\text{photons}}{\text{s}}$$
 (1.2b)

Ch01_Eqs1.1_2.ai

Lectures online at www.youtube.com





Amazon.com



UC Berkeley

www.coe.berkeley.edu/AST/sxreuv www.coe.berkeley.edu/AST/srms www.coe.berkeley.edu/AST/sxr2009